PHYSICAL REVIEW D **90,** 093001 (2014)

Electroweak form factors of the $\Delta(1232)$ resonance

Krzysztof M. Graczyk, Jakub Żmuda, and Jan T. Sobczyk

Institute of Theoretical Physics, University of Wrocław, plac Maxa Borna 9, 50-204 Wrocław, Poland

(Received 21 July 2014; published 3 November 2014)

Nucleon $\to \Delta(1232)$ transition electroweak form factors are discussed in a single pion production model with nonresonant background terms originating from a chiral perturbation theory. Fits to electron-proton scattering F_2 as well as neutrino scattering bubble chamber experimental data are performed. Both ν-proton and ν-neutron channel data are discussed in a unified statistical model. A new parametrization of the $N \to \Delta(1232)$ vector form factors is proposed. In the case of model with deuteron nuclear effects fit to neutrino scattering data gives the axial mass $M_{A\Delta} = 0.85^{+0.09}_{-0.08}$ GeV and $C_5^A(0) = 1.10^{+0.15}_{-0.14}$ in accordance with the Goldberger-Treiman relation. However, the consistency is spoiled when the deuteron effects are omitted; i.e., in this case the fit gives the axial mass $M_{A\Delta} = 0.81^{+0.09}_{-0.09}$ GeV and $C_5^A(0) = 0.93^{+0.13}_{-0.13}$.

DOI: 10.1103/PhysRevD.90.093001 PACS numbers: 13.15.+g, 13.60.Le

I. INTRODUCTION

Weak single pion production (SPP) processes have been studied for many decades, but their importance in neutrino physics has grown with the development of accelerator neutrino experiments. In the few-GeV energy range characteristic for the experiments such as T2K [1], MINOS [2], NOvA [3], MiniBooNE [4], and LBNE [5], this interaction channel contributes a large fraction of the total cross section. Rough estimates show that for an isoscalar target and neutrino energy of around 1 GeV, SPP accounts for about $1/3$ of the interactions.

The SPP events with pion absorption contribute to the background in measurements of quasielastic neutrino scattering on nuclear targets. Neutral current π^0 production processes add to the background for the ν_e appearance measurement in water Cherenkov detectors. The detailed estimate of the cross sections for the SPP is important for a correct extraction of neutrino oscillation parameters in long baseline experiments.

Theoretical modelling of the SPP processes on nuclear targets suffers from extra complications. Any attempt to obtain information about the nucleon (N) to $\Delta(1232)$ resonance transition vertex from these data is biased by systematic errors coming from nuclear model uncertainties. On the experimental side, there seems to be a tension between the MiniBooNE and very recent MINERνA SPP data on (mostly) carbon target (see Ref. [6]). For hereby analysis measurements of the neutrino-production on free or almost free targets are desired. At present such data exist only for the ~30-year-old Argonne National Laboratory (ANL) [7,8] and Brookhaven National Laboratory (BNL) [9,10] bubble chamber experiments, where deuteron and hydrogen targets were utilized. In this case one may hope to reduce the many-body bias in a reasonable manner with a simple theoretical ansatz [11].

In order to understand the neutrino SPP data it is necessary to have a model of nonresonant background (see Ref. [12]). In more recent studies of weak SPP typically only the neutrino-proton channel $\nu_\mu + p \to \mu^- + \pi^+ + p$ is discussed in detail [13–18]. This is a big drawback, because simple total cross section ratio analysis shows, that the background contribution is much larger in neutrino-neutron channels. The neutrino-proton SPP channel can be described well within a model that contains the $\Delta(1232)$ resonance contribution only (see, e.g., Ref. [19]). In the latter paper it was argued that the $d\sigma/dQ^2$ results in [8] do not include the flux normalization error. Incorporating into the analysis this error and also the deuteron effects in both ANL and BNL experiments allowed for a consistent fit for both data sets with $C_5^A(0) = 1.19 \pm 0.08$ and $M_A = 0.94 \pm 0.03$ GeV. The attempt to extract the leading $C_5^A(Q^2)$ $N \to \Delta$ form factor parameters in a model containing nonresonant background has been done in Refs. [14,16]. The results both for a model without [14] and with deuteron effects [16] gave the values of $C_5^A(0)$ far from the Goldberger-Treiman relation estimate of $C_5^A(0) \approx 1.2$ [20] ($C_5^A(0) = 0.867 \pm 0.075$ in [14] and $C_5^A(0) = 1.00 \pm 0.11$ in [16]). From the above-mentioned models, only those in Refs. [13,15] have been directly validated on the electroproduction processes. Some authors use vector form factor parametrization from Ref. [21], based on the MAID analysis [22]. The authors of Ref. [21] proposed a model containing only Δ resonance contribution without any background and compared it to the MAID2007 helicity amplitudes. The problem is that the Δ helicity amplitudes extraction procedure is model-dependent. There are important Δ-background interference effects and the separation procedure depends on the background model details. It is important to have the Δ form factors consistent with the other ingredients of the model.

Keeping in mind the above caveats of previous analyses we propose an improved approach. We adapt and develop the statistical framework of Ref. [19] in order to fit both vector and axial form factors of the $\Delta(1232)$ resonance. We use inclusive electron-proton scattering data for the electromagnetic interaction in the $\Delta(1232)$ region and deuteron

bubble chamber data for the weak one. For the latter we expand the previously used statistical approach in order to incorporate the neutron channels, which was never done before. In this manner we include the data sets, which are very sensitive to the nonresonant background.

This paper is organized as follows: Sec. II is devoted to the general formalism of single pion production, Sec. III introduces the statistical model of our analysis, Sec. IV shows our main results, and finally Sec. V contains the conclusions.

II. GENERAL FORMALISM

We discuss the charged current inelastic neutrino scattering off nucleon targets. Three channels for neutrino SPP interactions are:

$$\nu_\mu(l) + p(p) \to \mu^-(l') + \pi^+(k) + p(p') \tag{1}$$

$$\nu_\mu(l) + n(p) \to \mu^-(l') + \pi^0(k) + p(p') \tag{2}$$

$$\nu_\mu(l) + n(p) \to \mu^-(l') + \pi^+(k) + n(p') \tag{3}$$

with l, l', p, p', and k being the neutrino, muon, initial nucleon, final nucleon, and pion four-momenta, respectively. The four-momentum transfer is defined as

$$q = l - l' = p' + k - p, \qquad Q^2 = -q^2, \qquad q^\mu = (q^0, \mathbf{q}), \tag{4}$$

and the square of the hadronic invariant mass is

$$W^2 = (p+q)^2 = (p'+k)^2. \tag{5}$$

Throughout this paper the metric $g^{\mu\nu} = \mathrm{diag}(+,-,-,-)$ is used.

For the pion electroproduction we are interested in proton target reactions:

$$e^-(l) + p(p) \to e^-(l') + \pi^+(k) + n(p') \tag{6}$$

$$e^-(l) + p(p) \to e^-(l') + \pi^0(k) + p(p'). \tag{7}$$

In the 1-GeV G energy region the process (1) is overwhelmingly dominated by the intermediate $\Delta^{++}(1232)$ state. The dominance of the resonant pion production mechanism makes this channel attractive for the analysis of the $\Delta(1232)$ properties. The other two channels [Eqs. (2) and (3)] are known to have a large nonresonant pion production contribution and thus present more challenges for theorists.

A. Cross section

The inclusive double differential SPP cross section for neutrino scattering off nucleons at rest has the following form:

$$\begin{aligned}
\frac{d^2\sigma}{dQ^2 dW} &= \frac{4\pi^2}{E^2} G_F^2 \cos^2\theta_C \frac{W}{M} \int \frac{d^3k}{(2\pi)^3 2E_\pi(k)} L_{\mu\nu} H^{\mu\nu} \\
L^{\mu\nu} &= l^\mu l'^\nu + l^\nu l'^\mu - g^{\mu\nu} l\cdot l' + i\epsilon^{\mu\nu\alpha\beta} l'_\alpha l_\beta \\
H^{\mu\nu} &= \frac{1}{2}\int \frac{d^3p'}{(2\pi)^3} \frac{1}{4ME(p')} \sum_{\text{spins}} \langle \pi N' | j^\mu_{cc}(0) | N\rangle \\
&\quad \times \langle \pi N' | j^\nu_{cc}(0) | N\rangle^* \delta^{(4)}(p' + k - p - q) \\
&= \frac{1}{128\pi^3 ME(p')} A^{\mu\nu} \delta(E(p') + E_\pi(k) - M - q^0),
\end{aligned} \tag{8}$$

where E is incident neutrino energy, M is the averaged nucleon mass, $E_\pi(k)$ and $E(p')$ are the final state pion and nucleon energies, $G_F = 1.1664 \times 10^{-11}$ MeV^{-2} is the Fermi constant, $L^{\mu\nu}$ the leptonic tensor, and $H^{\mu\nu}$ the hadronic tensor. The Cabibbo angle, $\cos(\theta_C) = 0.974$, was factored out of the weak charged current definition.

The information about the dynamics of SPP is contained in matrix elements, $\langle \pi N' | j^\mu_{cc}(0) | N\rangle$, which describe the transition between an initial nucleon state $|N>$ and a final nucleon-pion state $|\pi N'>$. One can introduce "reduced current matrix elements" s^μ and express the weak transition amplitudes,

$$\langle N'(p',s')\pi(k) | j^\mu_{cc} | N(p,s)\rangle = \bar{u}_{p'}(s') s^\mu u_p(s), \tag{9}$$

with isospin information hidden inside s^μ.

After performing the summations over nucleon spins, we can rewrite the hadronic tensor as

$$A^{\mu\nu} = \mathrm{Tr}[(\not{p}' + M) s^\mu (\not{p} + M) \gamma^0 s^{\nu\dagger} \gamma^0], \tag{10}$$

where $\not{p} = \gamma_\mu p^\mu$.

The differential cross section on free nucleons becomes then

$$\begin{aligned}
\frac{d^2\sigma}{dW dQ^2} &= \frac{G_F^2 \cos^2(\Theta_C)}{512\pi^4 E^2 M} \int d\Omega_\pi \int_0^\infty \frac{\mathbf{k}^2 d|k|}{E_\pi(k) E(p')} \\
&\quad \times \frac{W}{M} L_{\mu\nu} A^{\mu\nu} \delta(E(p') + E_\pi(k) - M - q^0).
\end{aligned} \tag{11}$$

In the model of this paper the dynamics of SPP process is defined by a set of Feynman diagrams (Fig. 1) with vertices determined by the effective chiral field theory. They are discussed in Ref. [14], where one can find exact expressions for s^μ. The same set of diagrams describes also pion electroproduction, with the exception of the pion pole diagram, which is purely axial. We call this approach the "HNV model" after the names of the authors of Ref. [14].

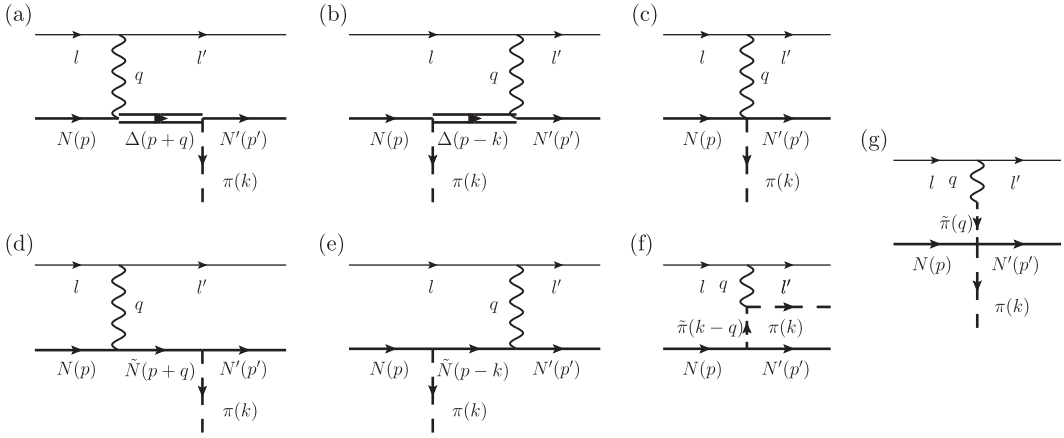

FIG. 1. Basic pion production diagrams from [14]: (a) Delta pole (ΔP), (b) crossed Delta pole (CΔP), (c) contact term (CT), (d) nucleon pole (NP), (e) crossed nucleon pole (CNP), (f) pion-in-flight (PIF), (g) pion pole (PP).

B. $N \to \Delta(1232)$ excitation

The $\Delta(1232)$ resonance excitation is treated within the isobar framework. For positive parity spin-$\frac{3}{2}$ particles we can write down a general form of the electroweak excitation vertex:

$$\Gamma^{\alpha\mu}(p,q) = [V^{\alpha\mu}_{3/2} - A^{\alpha\mu}_{3/2}]\gamma^5,$$

where

$$V^{\alpha\mu}_{3/2} = \frac{C_3^V(Q^2)}{M}(g^{\alpha\mu}\not{q} - q^\alpha\gamma^\mu) + \frac{C_4^V(Q^2)}{M^2}(g^{\alpha\mu}q\cdot(p+q) - q^\alpha(p+q)^\mu) + \frac{C_5^V(Q^2)}{M^2}(g^{\alpha\mu}q\cdot p - q^\alpha p^\mu) + g^{\alpha\mu}C_6^V(Q^2) \tag{12}$$

$$-A^{\alpha\mu}_{3/2} = \left[\frac{C_3^A(Q^2)}{M}(g^{\alpha\mu}\not{q} - q^\alpha\gamma^\mu) + \frac{C_4^A(Q^2)}{M^2}(g^{\alpha\mu}q\cdot(p+q) - q^\alpha(p+q)^\mu) + C_5^A(Q^2)g^{\alpha\mu} + \frac{C_6^A(Q^2)}{M^2}q^\alpha q^\mu\right]\gamma^5. \tag{13}$$

A relevant information about the inner structure of the $\Delta(1232)$ resonance is contained in a set of vector and axial form factors, $C_j^{V,A}$ assumed to be functions of Q^2 only (with the exception of C_4^V which depends also on W).

C. Conserved vector current and vector form factors

Thanks to conserved vector current (CVC) hypothesis we can express weak vector form factors by electromagnetic ones. There exist several parametrizations of C_j^V proposed over the course of past five decades (see Refs. [21–24]). In this paper we propose our own model in order to be consistent with the chosen description of the nonresonant background. The size and excellent accuracy of the electromagnetic data set allows for an introduction of multiple fit parameters.

We assume that the $N \to \Delta$ transition form factors have the same large Q^2 behavior as the electromagnetic elastic nucleon form factors. The theoretical arguments [25] suggest that at $Q^2 \to \infty$ the nucleon form factors fall down as $1/Q^4$ and we adopt appropriate Padé type parametrization used previously to parametrize the electromagnetic form factors of the nucleon [26]. We allow for a deviation from the $SU(6)$-symmetry quark model relations $C_4^V(Q^2) = -\frac{M}{W}C_3^V(Q^2)$ and $C_5^V = 0$ between the form factors [27]. Finally, to reduce the number of parameters in C_5^V we assume the dipole representation. Altogether, our parametrization has the following form:

$$C_3^V(Q^2) = \frac{C_3^V(0)}{1 + AQ^2 + BQ^4 + CQ^6}\cdot(1 + K_1Q^2) \tag{14}$$

$$C_4^V(Q^2) = -\frac{M_p}{W}C_3^V(Q^2)\cdot\frac{1 + K_2Q^2}{1 + K_1Q^2} \tag{15}$$

$$C_5^V(Q^2) = \frac{C_5^V(0)}{(1 + D\frac{Q^2}{M_V^2})^2}. \tag{16}$$

We use the standard value of the vector mass $M_V = 0.84$ GeV. This parametrization reproduces the quark model relation between C_3^V and C_4^V at $Q^2 = 0$ and is consistent with nonzero $S_{1/2}$ helicity amplitude.

In Sec. IV we present the best-fit values of parameters $C_3^V(0)$, $C_5^V(0)$, A, B, C, D, K_1 and K_2.

D. Partially conserved axial current and axial form factors

In the axial part the leading contribution comes from $C_5^A(Q^2)$ which is an analogue of the isovector nucleon axial form factor. Partially conserved axial current (PCAC) hypothesis relates the value of $C_5^A(0)$ with the strong coupling constant f^* through off-diagonal Goldberger-Treiman relation [20],

$$C_5^A(0) = \frac{f^*}{\sqrt{2}} \approx 1.2, \tag{17}$$

but we will treat $C_5^A(0)$ as a free parameter. Most often it is assumed, that C_5^A has a dipole Q^2 dependence:

$$C_5^A(Q^2) = \frac{C_5^A(0)}{(1+Q^2/M_{A\Delta}^2)^2}. \tag{18}$$

The axial mass parameter $M_{A\Delta}$ is expected to be of the order of 1 GeV. The authors of Refs. [14] and [17] use the parametrization of $C_5^A(Q^2)$ proposed in Ref. [28]:

$$C_5^A(Q^2) = \frac{C_5^A(0)}{(1+Q^2/M_{A\Delta}^2)^2}\frac{1}{(1+Q^2/(3M_{A\Delta}^2))^2}. \tag{19}$$

Other groups, e.g., the authors of Ref. [29], occasionally use parametrization from Ref. [30], which contains even more free parameters. In our fits we assume the dipole form of C_5^A.

The C_6^A form factor is an analogue of the nucleon induced pseudoscalar form factor. It can be related to C_5^A as

$$C_6^A(Q^2) = \frac{M^2}{m_\pi^2+Q^2} C_5^A(Q^2), \tag{20}$$

where m_π is average pion mass. The $C_3^A(Q^2)$ is the axial counterpart of the very small electric quadrupole (E2) transition form factor and we set $C_3^A = 0$. For the C_4^A we use the Adler model relation [31]:

$$C_4^A(Q^2) = -\frac{1}{4} C_5^A(Q^2). \tag{21}$$

In this way the axial contribution is fully determined by $C_5^A(Q^2)$. Altogether there are two free parameters: $C_5^A(0)$ and $M_{A\Delta}$. If there were enough experimental data one could drop the Adler relation and treat $C_4^A(Q^2)$ as an independent form factor. However, the ANL and BNL experimental data do not have sufficient statistics to obtain separate fits of C_5^A and C_4^A [32] (see also the discussion in Ref. [16]).

E. Deuteron effects

In this paper we consider a deuteron model based on phenomenological nucleon momentum distribution. The following effects are taken into account:

(i) Nucleon momentum distribution $f(p)$ taken from the Paris potential [33] (also used by the authors of Ref. [16]). We verified that other parameterizations (Hulthen [34], Bonn [35]) lead to very similar results.

(ii) *Flux correction* coming from varying relative neutrino-nucleon velocity,

$$v_{\rm rel} = \frac{\sqrt{(l\cdot p)^2}}{EE(p)} = \left|\frac{(EE(p) - \mathbf{l}\cdot\mathbf{p})}{EE(p)}\right| = \left|1 - \frac{\mathbf{l}\cdot\mathbf{p}}{EE(p)}\right|. \tag{22}$$

(iii) Realistic energy balance within plane wave impulse approximation (PWIA). It is assumed that the spectator nucleon does not participate in the interaction. In the case of quasielastic neutrino scattering it was shown in [36] that for neutrino energies larger than 500 MeV final state interactions effects violating PWIA are very small. The effective, momentum dependent, binding energy becomes

$$B(p) = 2E(p) - M_D, \tag{23}$$

where M_D is deuteron mass.

(iv) De Forest treatment of the off-shell matrix elements [37].

The expression for the cross section becomes

$$\frac{d\sigma}{dQ^2 dW} = \int d^3p \frac{f(p)}{v_{\rm rel}} \frac{G_F^2 \cos^2(\Theta_C)|\mathbf{l}'|}{16\pi E_\nu E(p)|\mathcal{J}|} \int \frac{d^3k}{(2\pi)^3 2E_\pi(k)} \int \frac{d^3p'}{(2\pi)^3 2E(p')} L_{\mu\nu} A^{\mu\nu}(p,\tilde{q},k)\delta^4(p+\tilde{q}-k-p'). \tag{24}$$

with $\tilde{q}^\mu = (q^0 - B(p), \vec{q})$ and

$$\mathcal{J} = \mathrm{Det}\begin{pmatrix} \frac{\partial Q^2}{\partial\cos(\Theta)} & \frac{\partial Q^2}{\partial q^0} \\ \frac{\partial W}{\partial\cos(\Theta)} & \frac{\partial W}{\partial q^0} \end{pmatrix}. \tag{25}$$

The explicit form of the Jacobian $\mathcal{J}$ is complicated because the invariant mass W depends both on the energy transfer q^0 and the lepton scattering angle Θ.

III. STATISTICAL FRAMEWORK

Our main goal is to have a SPP model working for the weak pion production. A natural procedure is to extract the information about vector and axial form factors independently using first respective electron scattering and then neutrino SPP data. In the next paragraphs we describe details of our statistical model.

A. Vector contribution to weak SPP

The available electron data set is very prolific and accurate compared to the neutrino data. One can extract the information about the functional form of the vector $N \to \Delta$ transition form factors from several observables, including electron or target polarizations. Dedicated electroproduction experiments were performed in JLab and Bonn [38–42]. Our main goal (due to the poor quality of the neutrino SPP data) is to reproduce correctly only the most important characteristics of the neutrino SPP reactions: overall cross sections and distributions in Q^2. Detailed analysis of the electroproduction data should focus on pion angular distributions but it goes beyond the scope of this paper and is going to be a subject of further studies.

We explore the information contained in electron-proton F_2 data from [43]. In our fit we include 37 separate series (for different Q^2 values) of F_2 data points. Since our final analysis aims at neutrino ANL experiment we have restricted ourselves to data points from the lowest value of Q^2 (0.225 GeV^2) up to 2.025 GeV^2 only.

The data are for the inclusive structure function; thus, we have limited ourselves to values of invariant mass W up to $M_p + 2m_\pi$. Beyond that value the experimental data include more inelastic channels, starting from two pion production. Even with this limitation for $Q^2 \leq 2.025$ and $W < M_p + 2m_\pi$ there are still 603 data points.

In order to ensure that the results will reproduce well the data at the $\Delta(1232)$ peak, we decided to expanded our fit to $W = 1.27$ GeV. Because there are no exclusive electron SPP data in the region $W \in (M + 2m_\pi, 1.27\ \text{GeV})$, we add to our fit a term in which MAID 2007 model predictions are taken as 228 fake data points. The total errors are identical with those of respective Osipenko *et al.* [43] points. Additional points help to reproduce better the $\Delta(1232)$ peak region. From technical reasons we could not apply the MAID model directly in our fits (the exact formulas for their SPP amplitudes have never been published). We have generated these additional points using the on-line version of MAID (http://wwwkph.kph.uni-mainz.de/MAID//). We have also used an information about MAID 2007 model helicity amplitudes. The caveat is that the experimental results contain both resonant and nonresonant contributions (see, e.g., Ref. [44]). Thus the measured helicity amplitudes depend on how one defines the "Delta" and "background." The HNV model differs with MAID in the treatment of both and one cannot expect the extracted helicity amplitudes to be the same. The information about helicity amplitudes enters our estimator with a large *ad hoc* error assumption.

B. Axial contribution to weak SPP: Neutrino bubble chamber experiments

We consider a statistical framework, proposed in Ref. [19], which incorporates the relevant data from the ANL experiment and allows for a treatment of both $C_5^A(0)$ and $M_{A\Delta}$ as free parameters.

The main results of the ANL experiment were published in Refs. [7,8]. ANL used a neutrino beam with mean energy below 1 GeV and a large flux normalization uncertainty $\Delta p_{\text{ANL}} \sim 20\%$ that was not included in the published $d\sigma/dQ^2$ cross section for the reaction in Eq. (1) [19]. ANL reported the data with the invariant mass cut $W < 1.4$ GeV, which allows us to confine to the $\Delta(1232)$ region and neglect contributions from heavier resonances, whose axial couplings are by large unknown. Our analysis uses information from both proton and neutron SPP channels.

In the $\nu_\mu + p \to \mu^- + p + \pi^+$ channel (denoted as A1), there are data on flux-averaged differential cross section σ_i^{exp} with respect to Q^2. The ANL papers provide their errors, $\Delta\sigma_i^{\text{exp}}$. By looking at the corresponding numbers of detected events one can show that $\Delta\sigma_i^{\text{exp}}$ are statistical errors only. Following [19] we explore this fact and make the analysis more complete by considering also a correlated error coming from the overall flux normalization uncertainty. We define the χ^2 estimator as

$$\chi^2_{A1} = \sum_{i=1}^{9} \left(\frac{\sigma_i^{\text{th}} - p_{\text{ANL}} \cdot \sigma_i^{\text{exp}}}{p_{\text{ANL}} \Delta\sigma_i^{\text{exp}}} \right)^2 + \left(\frac{p_{\text{ANL}} - 1}{\Delta p_{\text{ANL}}} \right)^2 \quad (26)$$

with ANL normalization factor p_{ANL} treated as a free parameter.

The theoretical cross sections are defined as

$$\sigma_i^{\text{th}} = \frac{1}{\Delta Q_i^2} \frac{1}{\int_{E_{\text{min}}}^{E_{\text{max}}} \Phi(E') dE'} \int_{Q_i^2 - \Delta Q_i^2/2}^{Q_i^2 + \Delta Q_i^2/2} dQ^2 \int_{E_{\text{min}}}^{E_{\text{max}}} dE \Phi(E) \cdot \frac{d\sigma^{\text{th}}(E, Q^2)}{dQ^2}, \quad (27)$$

$$\frac{d\sigma^{\rm th}(E,Q^2)}{dQ^2} = \int_{M+m_\pi}^{1.4\ {\rm GeV}} dW \frac{d^2\sigma^{\rm th}(E,Q^2)}{dW dQ^2}. \quad (28)$$

Q_i^2 is the ith bin central Q^2 value, ΔQ_i^2 is the bin width, and $\Phi(E)$ is the ANL flux. In this channel the integral spans neutrino energies between $E_{\rm min} = 0.5$ and $E_{\rm max} = 6$ GeV.

For both ANL neutron channels $\nu_\mu + n \to \mu^- + p + \pi^0$ (denoted as A2) and $\nu_\mu + n \to \mu^- + n + \pi^+$ (denoted as A3) the data are in a form of event distributions in Q^2 denoted as $N_i^{\rm EXP}$ and also a few overall cross sections points. In our study we include experimental correction factors $C^{\rm exp}$, $N_j^{\rm exp} \to C^{\rm exp} N_j^{\rm exp}$, together with their uncertainties $\delta C^{\rm exp}$ (Table I in [8]). These correction factors are related to detector efficiencies and multiple kinematic cuts. We define estimator for both neutron channels as

$$\chi^2_{A2,3} = \sum_{i=1}^{N_{A2,3}} \frac{\left(\frac{\sigma^{\rm th}_{A2,3;i}}{\sigma^{\rm th}_{A2,3,{\rm tot}}} N^{\rm exp}_{A2,3} p_{\rm ANL} - N^{\rm exp}_{A2,3;i}\right)^2}{N_i^{\rm exp}} + \left(\frac{\frac{\sigma^{\rm th}_{A2,3,{\rm tot}}}{\sigma^{\rm exp}_{A2,3,{\rm tot}} \cdot p_{\rm ANL}} - 1}{\Delta p_{\rm ANL}}\right)^2, \quad (29)$$

where

$$N^{\rm exp}_{A2,3} = \sum_{j=1}^{12} N^{\rm exp}_{A2,3;j} \quad (30)$$

$$\sigma^{\rm th}_{A2,3,{\rm tot}} = \sum_{j=1}^{12} \sigma^{\rm th}_{A2,3;j} \quad (31)$$

$\sigma^{\rm exp}_{A2,3,{\rm tot}}$ is the total cross section for the $A2,3$ channel, and $N^{\rm exp}_{A2,3;i}$ is the number of events in the ith bin of the $A2,3$ channels.

Some of the experimental bins contain too few events for an χ^2-based analysis. We have combined some of the neighboring bins in order to keep a meaningful event statistics and the number of Q^2 bins is 12 in both neutron channels. The upper bound on neutrino energy is now $E_{\rm max} = 1.5$ GeV and one has to account for that fact by changing the integration limits and normalization factor in Eq. (27).

Eventually, the complete χ^2 function for the ANL data reads

$$\chi^2_{\rm ANL} = \sum_{k=1}^{3} \chi^2_{Ak}. \quad (32)$$

IV. RESULTS

A. Electromagnetic fits

The best-fit results of our vector form factor parametrization given by Eqs. (14)–(16) are shown in Table I. For our best-fit the value of $C_3^V(0)$ is close to the one from Ref. [21] and we get a clear beyond-dipole Q^2 dependence of $C_3^V(Q^2)$ and $C_4^V(Q^2)$. Surprisingly, the Q^2 dependence of $C_5^V(Q^2)$ is exactly dipole $(1 + Q^2/M_V^2)^{-2}$ with $M_V = 0.84$ GeV being the standard vector mass.

TABLE I. Best-fit coefficients for vector form factors given by Eqs. (14)–(16) to be used in neutrino scattering data analysis. We do not report 1σ errors because of hybrid character of our estimator (see explanations in the text).

$C_3^V(0)$	$C_5^V(0)$	A	B	C	D	K_1	K_2
2.10	0.63	4.73	−0.39	5.59	1.00	0.13	1.68

Figure 2 shows that qualitatively in the region below two pion production threshold our fit reproduces the data rather well. In the same figure we show also predictions from the MAID2007 model. In order to compare both results we calculated the χ^2 contribution from data points below the 2π threshold ($\chi^2_{<2\pi}$). The same χ^2 function with the MAID2007 model predictions gives $\chi^2_{W<M_p+2m_\pi}/{\rm NDF} \approx 12.1$ and with our best-fit results-$\chi^2_{W<M_p+2m_\pi}/{\rm NDF} \approx 13.6$. Our form factors lead to better agreement with the electron scattering data than the form factors considered in Ref. [21] (with the same HNV background model) giving $\chi^2_{W<M_p+2m_\pi}/{\rm NDF} = 16.5$. Inspection of Fig. 2 (and also similar figures not shown in the paper) shows that most of the contribution to χ^2 comes from a region of low W. Our fits are going to be used in the analysis of neutrino

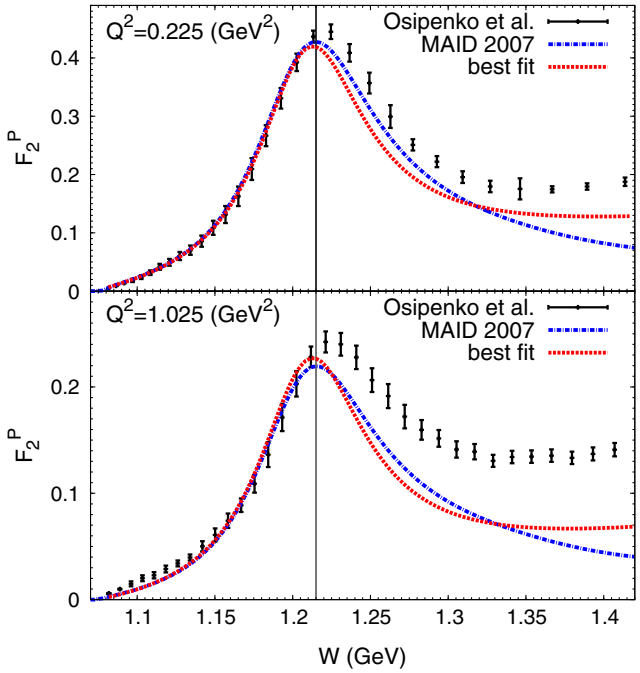

FIG. 2 (color online). Best-fit results for vector form factors given by Eqs. (14)–(16) plotted against experimental data from Ref. [43] as well as MAID2007 predictions. Vertical lines show the 2π production threshold.

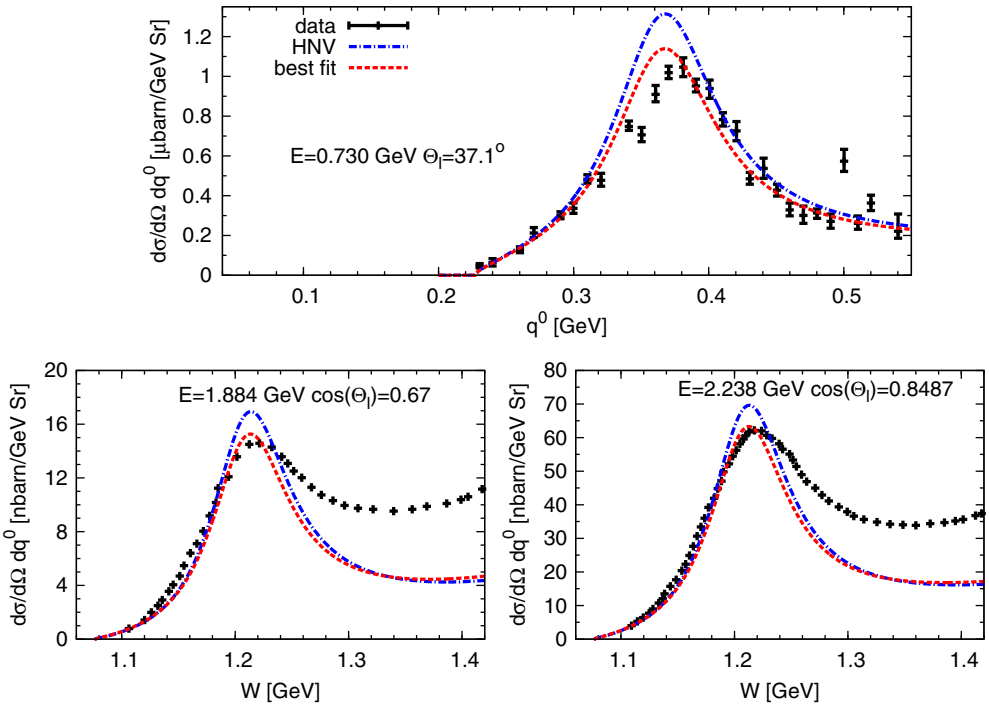

FIG. 3 (color online). Comparison of our best fit and the HNV model with Lalakulich-Paschos form factors of Ref. [21] plotted against inclusive $p(e,e')$ data (not included in the fit) from Ref. [45] (top) and Ref. [46] (bottom). The Q^2 values at peak are from top to bottom and left to right: 0.1, 1.15, and 0.95 GeV^2, respectively.

scattering data and some discrepancy at low W is of no practical importance.

Figure 3 shows an example of the performance of our best fit and form factors from Ref. [21] with the same background. Our model gives results closer to the experimental data than the form factors proposed in Ref. [21].

B. Axial fits

For the axial contribution to $N \to \Delta$ transition our analysis assumes, that $C_5^A(0)$, $M_{A\Delta}$ and normalization factor p_{ANL} are free fit parameters. We present our results in Table II and in Figs. 4 and 5.

In Table II are the results for fits to all three channels separately, and also the joint fit to three channels together. In each case the number of degrees of freedom is calculated as NDF = No. Q^2 bins − No. fitted parameters. In order to illustrate a role of deuteron effects we show also the results for a "model" of deuteron as consisting from free proton and neutron.

In both the free target and deuteron target cases, we see that taken separately the $p\pi^+$ (A1) and $p\pi^0$ (A2) channels

TABLE II. Best-fit for the Δ(1232) axial form factors. Upper table: free nucleon target, lower table: deuteron target. 1σ contours for physical parameters can be found in Figs. 4 and 5. Errors for $C_5^A(0)$ and $M_{A\Delta}$ where obtained after marginalization of p_{ANL}.

	Fit	$C_5^A(0)$	$M_{A\Delta}$ (GeV)	p_{ANL}	χ^2/NDF	NDF
Free n + p	A1	$0.94^{+0.30}_{-0.30}$	$0.93^{+0.18}_{-0.19}$	1.03	0.15	6
	A2	$1.09^{+0.50}_{-0.69}$	$0.94^{+0.30}_{-0.30}$	0.93	1.55	9
	A3	$2.48^{+0.52}_{-0.52}$	$0.75^{+0.14}_{-0.14}$	0.94	1.56	9
	Joint	$0.93^{+0.13}_{-0.13}$	$0.81^{+0.09}_{-0.09}$	0.89	2.11	30
Deuteron	A1	$1.11^{+0.32}_{-0.34}$	$0.97^{+0.17}_{-0.17}$	1.04	0.20	6
	A2	$1.31^{+0.49}_{-0.77}$	$1.00^{+0.27}_{-0.25}$	0.93	1.52	9
	A3	$2.83^{+0.62}_{-0.60}$	$0.76^{+0.13}_{-0.13}$	0.94	1.47	9
	Joint	$1.10^{+0.15}_{-0.14}$	$0.85^{+0.09}_{-0.08}$	0.90	2.06	30

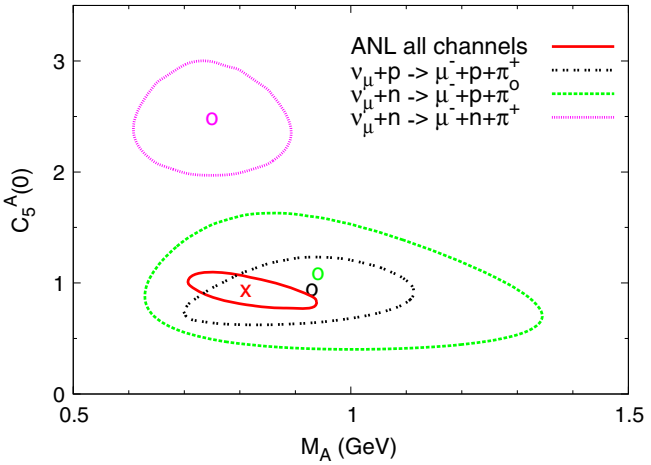

FIG. 4 (color online). 1σ uncertainty contours for fits on the free target.

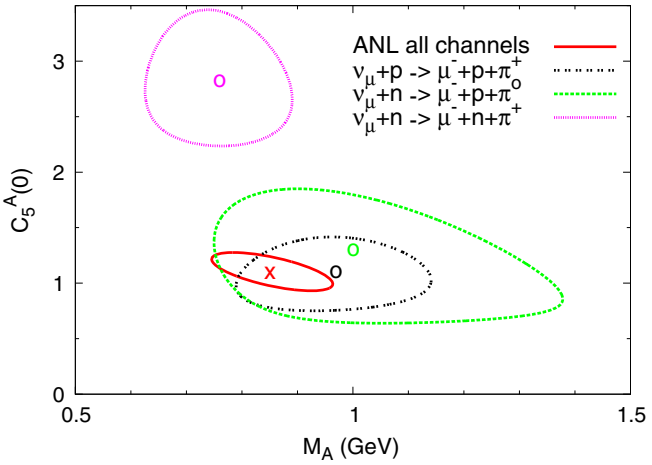

FIG. 5 (color online). 1σ uncertainty contours for fits on the deuteron target.

are statistically consistent, although their predicted scale parameters differ by around 10%. The latter channel seems to carry less information on the $N \to \Delta$ transition axial current than the first one, which is reflected in larger uncertainty contours. This could be explained by a bigger background contribution to that channel, which makes it less sensitive to changes in the Δ resonance description.

The biggest difficulty is encountered in the $n\pi^+$ (A3) channel, where we obtain $C_5^A(0)$ twice as large as for the other two channels and $M_{A\Delta}$ significantly smaller. Here the number of events reported by ANL is comparable to $p\pi^0$ channel, but theoretical cross section predictions with nonresonant background are smaller, as one can readily see in Fig. 6. This results in the drastic overestimation of $C_5^A(0)$. Still, the fits to separate isospin channels give acceptable values of χ^2_{min} for both neutron channels.

Deuteron effects affect mostly the value of $C_5^A(0)$, by up to 20% depending on interaction channel. The same applies to the joint fit. A significant improvement with respect to previous fits to the HNV model done in Refs. [14,16] is that with deuteron target effects, we get the best-fit value of $C_5^A(0)$ within 1σ range from the theoretical Goldberger-Treiman relation. The joint fit agrees also on the 1σ level with separate fits on $p\pi^0$ and $p\pi^+$ channels. Deuteron effects lead to a slight improvement in the values of χ^2_{min}.

We have compared total cross section and Q^2 event distribution from the ANL experiment and our best fit. They are presented in Figs. 6 and 7, respectively. They reflect previously described problems with the $n\pi^+$ channel. For two other channels we get a good agreement with the data.

Fitted normalizations factors p_{ANL} are different for neutron and proton channel as long as one considers separate fits. The proton channel prefers the data to be scaled up and both neutron channels prefer the data to be scaled down. Inclusion of deuteron effects does not change the value of fitted p_{ANL}. The joint fit uses the same p_{ANL}

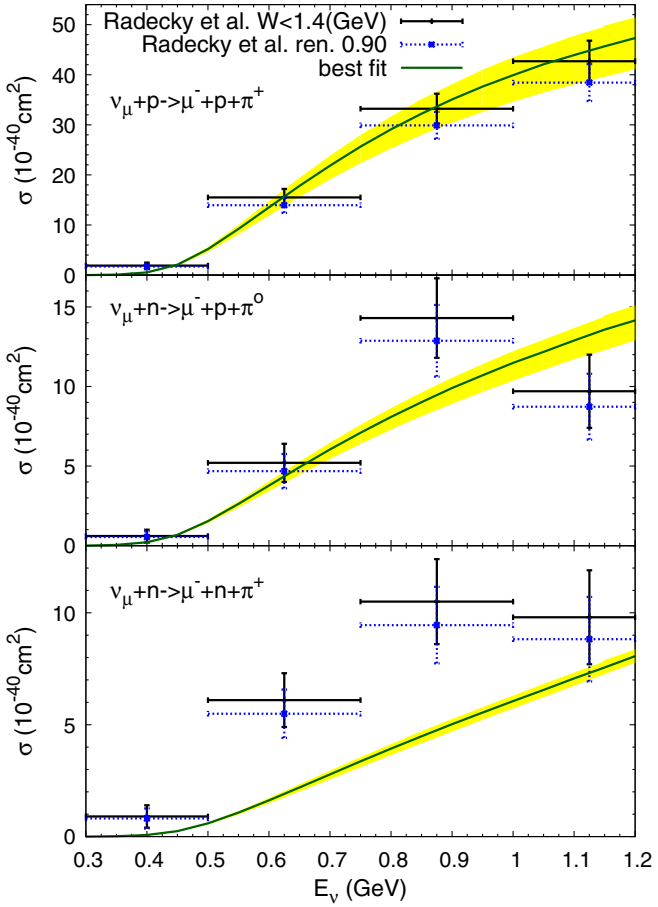

FIG. 6 (color online). Total cross sections for our best-fit form factors on the deuteron target with 1σ error bands. Black/solid lines represent the experimental data from Ref. [8]; blue/dotted lines represent the same data multiplied by the best-fit value of $p_{\text{ANL}} = 0.90$ (see Table II).

parameter for all channels and seems to prefer the data to be scaled down even more ($p_{\text{ANL}} \approx 0.90$ both for free and deuteron targets). These values of p_{ANL} are all well within the assumed error Δp_{ANL}. This indicates that our fitting procedure is numerically stable. The effect of the fitted overall normalization factor has been shown in Fig. 6 for the total cross sections and in Fig. 7 for the differential cross sections.

Finally, we noticed that the best fit values for $C_5^A(0)$ and $M_{A\Delta}$ are different from those obtained in Ref. [19] because in the current analysis the nonresonant background contribution is included.

C. Inclusion of BNL data

We repeated the similar analysis with the BNL SPP data published in [9] and [10]. The BNL neutrino flux was of somewhat higher energy than ANL, $\langle E \rangle \approx 1.6$ GeV, with flux uncertainty $\Delta p_{\text{BNL}} \approx 10\%$ (see Ref. [19]). For our purposes, the most useful data are for the $\nu_\mu + p \to \mu^- + p + \pi^+$ reaction in a form of distribution of events with a

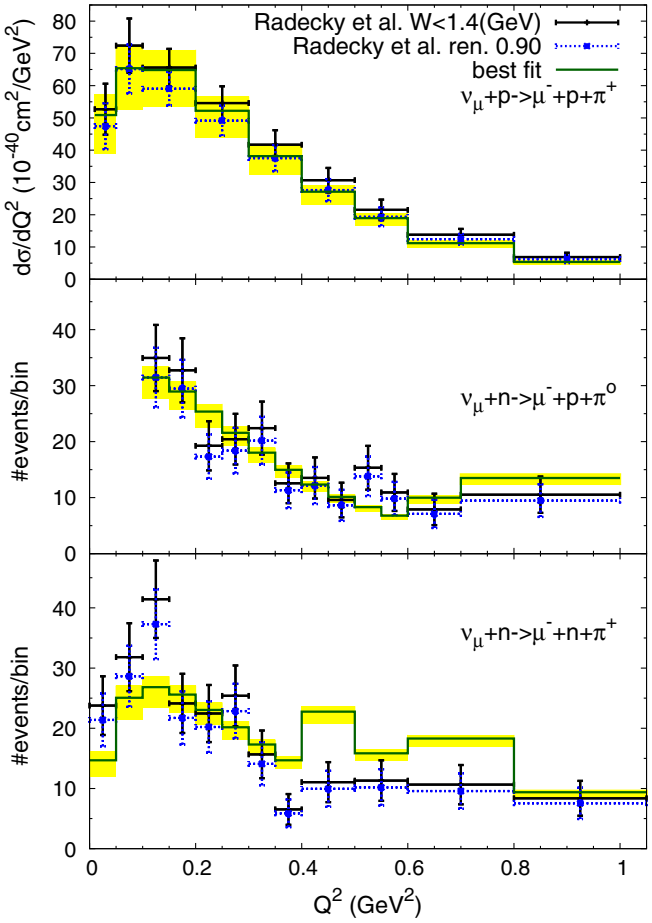

FIG. 7 (color online). The ANL Q^2 cross section and event distributions for our best fit and deuteron target. Black/solid lines represent the experimental data from Ref. [8]; blue/dotted lines represent the same data multiplied by the best-fit value of $p_{\mathrm{ANL}} = 0.90$ (see Table II).

cut $W < 1.4$ GeV. Neutron channel results have been reported without a W cut and they contain a large contamination coming from heavier resonances. We used the same formula for χ^2 function as in Ref. [19], Sec. 5.2 with the normalization factor for the BNL data, p_{BNL}, treated as a free fit parameter.

The joint ANL+BNL data fit was done for the $p\pi^+$ channel and the best fit result is: $C_5^A(0) = 1.26^{+0.20}_{-0.21}$ (consistent with Goldberger-Treiman relation) and $M_{A\Delta} = 1.06^{+0.10}_{-0.09}$ GeV ($\chi^2/\mathrm{NDF} = 0.74$ with $\mathrm{NDF} = 35$), see Fig. 8. Our results are different from those obtained in Ref. [16] because both studies use distinct estimators χ^2. In Ref. [16] only total cross section information from the BNL data is utilized. As explained above, we have used an information from the shape of Q^2 event distributions as well. In the study in Ref. [16] most of the data points come from the ANL experiment and joint best fit value of $C_5^A(0)$ becomes smaller.

We have obtained slightly different results from the ones from Ref. [19] ($C_5^A(0) = 1.19^{+0.08}_{-0.08}$ and $M_{A\Delta} = 0.94^{+0.03}_{-0.03}$ GeV), where the same χ^2 definition was used. Reasons for this are that we

(i) included the nonresonant background,
(ii) used new vector form factors,
(iii) and incorporated a better description of deuteron effects. In Ref. [19] an effective treatment of deuteron effects based on [11] was applied.

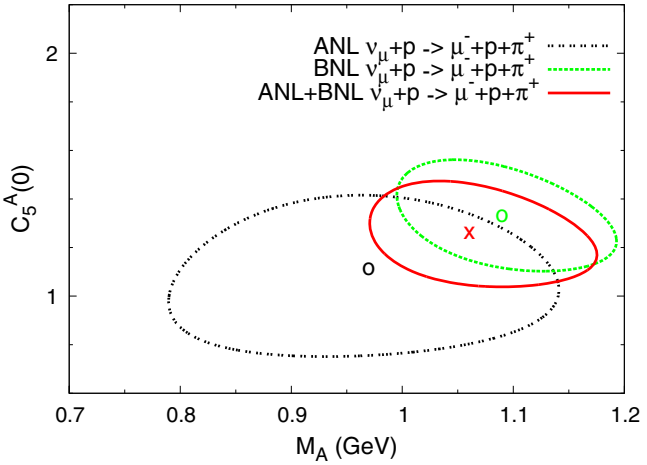

FIG. 8 (color online). Best-fit results for the ANL + BNL $p\pi^+$ data on deuteron target with 1σ error bands.

V. CONCLUSIONS

In this paper we made a new attempt to get an information about weak $N \to \Delta$ transition matrix elements. We first introduced new vector form factors, consistent with the HNV model of the nonresonant background. In the next step we investigated all three neutrino-free nucleon SPP channels, most importantly also neutrino-neutron channels that were never before used in the phenomenological studies.

Our main result is that the obtained value of $C_5^A(0)$ agrees, on the 1σ level, with the Goldberger-Treiman relation but only if the deuteron effects are taken into account. Indeed if one neglects the nuclear effects the resulting $C_5^A(0)$ value is lower. Also, our results confirm that there is a strong tension between $n\pi^+$ and the remaining two channels in the sense that the same theoretical model does not seem to reproduce all the data in a consistent way.

There can be various reasons for that. Those already mentioned include the following:

(i) ANL data for the neutron SPP channel have poor event statistics.
(ii) The HNV model for the background is well justified only near the pion production threshold and perhaps it is not reliable in the $\Delta(1232)$ peak region.

Still another reason for the theoretical difficulties may come from a missing unitarization of the model. The unitarity constraint, following the Watson theorem [47], imposes a relation between phases in weak neutrino-nucleon and pion-nucleon elastic scattering amplitudes not satisfied

in our approach. In a recent study Nieves, Alvarez-Ruso, Hernandez, and Vicente-Vacas [48] tried to correct the HNV model by introducing phenomenological phases in the leading multipole amplitude. This approach leads to a better agreement of the obtained best fit value of $C_5^A(0)$ with the Goldberger-Treiman relation. More theoretical studies in this direction are necessary.

Another observation is that SPP measurements with higher event statistics in the Δ region on proton or deuteron targets are badly needed. Keeping in mind the difficulties in the treatment of nuclear effects on heavier targets, it is the only way to get precise information about the $N \to \Delta$ axial transition matrix elements.

ACKNOWLEDGMENTS

We thank Luis Alvarez-Ruso for fruitful discussions. J. T. S. and J. Z. were supported by Polish National Science Centre Grant No. UMO-2011/M/ST2/02578. Numerical calculations were carried out in Wroclaw Centre for Networking and Supercomputing (http://www.wcss.wroc.pl), Grant No. 268.

[1] K. Abe *et al.* (T2K Collaboration), Nucl. Instrum. Methods Phys. Res., Sect. A **659**, 106 (2011).
[2] J. Evans (MINOS), Adv. High Energy Phys. **2013**, 182537 (2013).
[3] D. Ayres *et al.* (NOvA Collaboration), arXiv:hep-ex/0503053.
[4] A. Aguilar-Arevalo *et al.* (MiniBooNE Collaboration), Phys. Rev. Lett. **98**, 231801 (2007).
[5] C. Adams *et al.* (LBNE Collaboration), arXiv:1307.7335.
[6] O. Lalakulich, U. Mosel, and K. Gallmeister, Phys. Rev. C **86**, 054606 (2012).
[7] S. J. Barish, M. Derrick, T. Dombeck, L. G. Hyman, K. Jaeger, B. Musgrave, P. Schreiner, R. Singer *et al.*, Phys. Rev. D **19**, 2521 (1979).
[8] G. M. Radecky, V. E. Barnes, D. D. Carmony, A. F. Garfinkel, M. Derrick, E. Fernandez, L. Hyman, G. Levman *et al.*, Phys. Rev. D **26**, 3297 (1982); **26**, 3297(E) (1982).
[9] T. Kitagaki, H. Yuta, S. Tanaka, A. Yamaguchi, K. Abe *et al.*, Phys. Rev. D **34**, 2554 (1986).
[10] T. Kitagaki, H. Yuta, S. Tanaka, A. Yamaguchi, K. Abe, K. Hasegawa, K. Tamai, H. Sagawa *et al.*, Phys. Rev. D **42**, 1331 (1990).
[11] L. Alvarez-Ruso, S. Singh, and M. Vicente Vacas, Phys. Rev. C **59**, 3386 (1999).
[12] G. L. Fogli and G. Nardulli, Nucl. Phys. **B160**, 116 (1979).
[13] T. Sato, D. Uno, and T. Lee, Phys. Rev. C **67**, 065201 (2003).
[14] E. Hernandez, J. Nieves, and M. Valverde, Phys. Rev. D **76**, 033005 (2007).
[15] C. Barbero, G. Lopez Castro, and A. Mariano, Phys. Lett. B **664**, 70 (2008).
[16] E. Hernandez, J. Nieves, M. Valverde, and M. Vicente Vacas, Phys. Rev. D **81**, 085046 (2010).
[17] O. Lalakulich, T. Leitner, O. Buss, and U. Mosel, Phys. Rev. D **82**, 093001 (2010).
[18] B. D. Serot and X. Zhang, Phys. Rev. C **86**, 015501 (2012).
[19] K. M. Graczyk, D. Kielczewska, P. Przewlocki, and J. T. Sobczyk, Phys. Rev. D **80**, 093001 (2009).
[20] M. L. Goldberger and S. B. Treiman, Phys. Rev. **110**, 1178 (1958).
[21] O. Lalakulich, E. A. Paschos, and G. Piranishvili, Phys. Rev. D **74**, 014009 (2006).
[22] D. Drechsel, S. S. Kamalov, and L. Tiator, Eur. Phys. J. A **34**, 69 (2007).
[23] H. F. Jones and M. D. Scadron, Ann. Phys. (N.Y.) **81**, 1 (1973).
[24] A. Dufner and Y.-S. Tsai, Phys. Rev. **168**, 1801 (1968).
[25] S. J. Brodsky and G. R. Farrar, Phys. Rev. D **11**, 1309 (1975).
[26] J. Kelly, Phys. Rev. C **70**, 068202 (2004).
[27] J. Liu, N. C. Mukhopadhyay, and L.-s. Zhang, Phys. Rev. C **52**, 1630 (1995).
[28] E. A. Paschos, J. Y. Yu, and M. Sakuda, Phys. Rev. D **69**, 014013 (2004).
[29] M. Sajjad Athar, S. Chauhan, and S. K. Singh, Eur. Phys. J. A **43**, 209 (2010).
[30] P. A. Schreiner and F. Von Hippel, Nucl. Phys. **B58**, 333 (1973).
[31] S. L. Adler, Ann. Phys. (N.Y.) **50**, 189 (1968).
[32] K. M. Graczyk, *Proc. Sci.*, EPS-HEP (2009) 286 [arXiv:0909.5084].
[33] M. Lacombe, B. Loiseau, R. Vinh Mau, J. Cote, P. Pires, and R. de Tourreil, Phys. Lett., **101B**, 139 (1981).
[34] L. Hulthen and M. Sugawara, *Handbuch der Physik*, (Springer-Verlag, Berlin, 1957), Vol. 39.
[35] R. Machleidt, K. Holinde, and C. Elster, Phys. Rep. **149**, 1 (1987).
[36] G. Shen, L. Marcucci, J. Carlson, S. Gandolfi, and R. Schiavilla, Phys. Rev. C **86**, 035503 (2012).
[37] T. De Forest, Nucl. Phys. **A392**, 232 (1983).
[38] M. Ungaro *et al.* (CLAS Collaboration), Phys. Rev. Lett. **97**, 112003 (2006).
[39] K. Joo *et al.* (CLAS Collaboration), Phys. Rev. Lett. **88**, 122001 (2002).
[40] K. Joo *et al.* (CLAS Collaboration), Phys. Rev. C **68**, 032201 (2003).
[41] K. Joo *et al.* (CLAS Collaboration), Phys. Rev. C **70**, 042201 (2004).
[42] H. Egiyan *et al.* (CLAS Collaboration), Phys. Rev. C **73**, 025204 (2006).
[43] M. Osipenko, G. Ricco, M. Taiuti, M. Anghinolfi, M. Battaglieri *et al.*, arXiv:hep-ex/0309052.

[44] R. Davidson, N. Mukhopadhyay, and R. Wittman, Phys. Rev. D **43**, 71 (1991).
[45] J. S. O'Connell, W. R. Dodge, J. W. Lightbody, X. K. Maruyama, J. O. Adler, K. Hansen, B. Schroder, A. M. Bernstein *et al.*, Phys. Rev. Lett. **53**, 1627 (1984).
[46] M. Christy and P. E. Bosted, Phys. Rev. C **81**, 055213 (2010).
[47] K. M. Watson, Phys. Rev. **88**, 1163 (1952).
[48] L. Alvarez-Ruso, E. Hernandez, M. J. Vicente-Vacas, and J. Nieves, in Proc. of NuInt14, London, May 2014.